Desalination and Water Treatment
www.deswater.com
doi: 10.5004/dwt.2019.24732

170 (2019) 265–276
December

Synthesis of high-grade alumina from aluminium dross and its utilization for the sorption of radioactive cobalt

Mohamed Mahmoud E. Breky*, Emad Hassan Borai, Amany T. Kassem

Hot Laboratories and waste Management Center, Atomic Energy Authority, Cairo 13759, Egypt,
emails: chemist_elbreky@yahoo.com (M.M.E. Breky), emadborai@yahoo.com (E.H. Borai), amany.kassem@ymail.com(A.T. Kassem)

Received 28 February 2019; Accepted 26 July 2019

ABSTRACT

Aluminium dross (AD) forms on the surface of molten metal as the latter reacts with the furnace atmosphere and is usually considered a waste of aluminium production. AD contains a complex mixture of mostly aluminium oxide (AO), nitride, carbide and sulfide, some alloying elements and salts. Nevertheless, AD is considered as hazardous waste and a rich source of alumina. In the present study, waste dross rich in alumina was treated with either acid or base dissolution to recover alumina. Aluminium sulphate (AS) and AO were produced using sulfuric acid and sodium hydroxide leaching, respectively. AS sample was calcined at 500°C, 700°C and 900°C, individually. At 900°C, AS was thermally degraded and transformed into AO. Also AO, (AO/H_2SO_4) and (AO/HCl), was prepared using AD dissolution by NaOH and neutralized by dropwise addition of either 2 N H_2SO_4 (AO/H_2SO_4) or 2 N HCl (AO/HCl). The resulting samples were characterized by X-ray diffraction, X-ray fluorescence and scanning electron microscopy. The resulting samples produced from acid and base leaching were applied to remove a harmful radionuclide (Co^{2+}) from liquid waste. The maximum Co^{2+} adsorption capacity was 193, 180, 197, 296 and 235 mg g^{-1} for the as-prepared AS, where AS calcinated at 700°C, AO calcinated at 900°C, AO/HCl and AO/H_2SO_4, respectively.

Keywords: Aluminium dross; Alumina; Cobalt radionuclide; Removal capacity; Radioactive waste treatment

1. Introduction

The disposal and recycling of the dross produced by the aluminium industry are the global problems. Serious water pollution problems result from the leaching of toxic metal ions into ground water because the majority of dross is disposed of in landfill sites [1]. Furthermore, many noxious gases, such as NH_3, CH_4, PH_3, H_2 and H_2S, are emitted when aluminium dross (AD) comes in contact with water [1]. AD is formed by the natural oxidation of molten aluminium. When the metal is in contact with air, aluminium oxide (AO) forms on the outer surface of the melt. The residual metal in the dross is removed by re-melting the AD by adding a salt flux to minimize oxidation. The oxide in dross is present as a long continuous network in which aluminium is entrapped. The molten flux breaks this framework and facilitates the coalescence of aluminium drops that sink in the aluminium bath [2]. In most cases, a salt bath is used to maximize the recovery of aluminium. In this process, the oxide generation is less, but the resultant dross is toxic because of its salt content, making the disposal of dross and recovery of aluminium from dross more complex.

Drosses are classified into white and black dross according to their metal content. White dross has higher metal aluminium content and is produced from primary and secondary aluminium smelters; black dross has a lower metal content and is generated during aluminium recycling (secondary industry sector). White dross may contain from

* Corresponding author.

1944-3994/1944-3986 © 2019 Desalination Publications. All rights reserved.

15% to 70 % recoverable metallic aluminium and is a fine powder due to skimming molten aluminium. Black dross typically contains a mixture of AOs and slag with a recoverable aluminium content ranging from 12% to 18% and a much higher salt content (typically higher than 40%) than white dross. The non-metallic residues generated from dross smelting operations are often termed 'salt cake' and contain 3%–5% residual metallic aluminium [1].

Although aluminium production is highly energy intensive, dross recycling is very attractive from both energy and economic standpoints [3]. Recycling AD to obtain value-added products has received significant interest. The authors have demonstrated the conversion of AD to various high-value materials, including anion exchangers for the removal of toxic ionic substances [4–10] and adsorbents for gasses [11,12]. Murayama et al. [8] synthesized Mg–Al, Ca–Al and Zn–Al as layered double hydroxides using the AD leachates as a raw material and examined their performance as an anion exchanger. The Egyptalum Company (a major producer of aluminium in Egypt) generates approximately 12,800 tonnes of aluminium dross tailings (ADT) per year. ADT are aluminium-rich (45 wt.% Al) chemical waste and are currently neither properly dispensed nor adequately utilized [13]. In Egypt, large quantities of aluminium slag (dross) and moderate quantities of aluminium sludge are disposed of as waste by the aluminium industry, causing many ecological and health problems [14].

Sulfuric acid plays an important role in the aluminium process and has an interest in an alkaline acid, which allows it to quickly dissolve and increase the concentration of sulfate ions. Sulfuric acid will reduce the precipitation rate of aluminium sulfate and ensure the utilization of AD in a concentrated sulfuric acid solution. A sulfur ion concentration can be created in a solution, and the concentration depends on the availability of both acid and water to preserve dissolved aluminium sulfate during the solubility process [15].

Previously, sodium hydroxide is used for dissolving aluminium from bauxite, for opening monazite sand, and for leaching wolframite and scheelite ores [16,17]. Leaching by bases has the following advantages; (a) negligible corrosion problems, (b) suitability for ores containing carbonate gangue and (c) more selectivity, since iron oxides will not be leached out.

Previously, sodium hydroxide is used for dissolving aluminium from bauxite, for opening monazite sand, and for leaching wolframite and scheelite ores [16,17]

Alumina is one of the most important structural materials with several transition phases that have enormous technological and industrial significance [18]. Alumina is the most commonly used catalyst and catalyst support in heterogeneous catalysis due to its low cost, good thermal stability, high specific surface area, surface acidity and interaction with deposited transition metals. Alumina has eight different polymorphs – seven metastable phases (γ, k, p, η, θ and x) as well as the thermally stable α-phase. The metastable (also known as transition) phases of alumina are intrinsically nanocrystalline and can be easily synthesized by a variety of methods.

Al_2O_3 can be transformed into a different phase by heat treatment. Factors such as particle size, heating rate, impurities, and atmosphere may influence the sequence of phase transformations of alumina due to the effect on the kinetics of transformation [19–22]. According to Gitzen [23], γ-Al_2O_3 transforms to δ-Al_2O_3 when calcined above 800°C. The δ-Al_2O_3 transforms to θ-Al_2O_3 when calcined above 1,000°C. Finally, θ-Al_2O_3 transforms to α-Al_2O_3 when calcined above 1,100°C. However, the presence of impurities alters the barrier of phase transformations. For example, calcinations of γ-Al_2O_3 with 3% platinum impurity can cause the α-Al_2O_3 to form below 1,100°C [23–25].

Boehmite, aluminium oxyhydroxide (AlO(OH)), is a versatile material employed in sol–gel ceramics, surface coatings, rheology control applications, and pharmaceuticals [14]. It is also an important precursor for preparing alumina. γ-Al_2O_3 is commonly produced from boehmite by calcination at 500°C in air [26]. Amer [14] produced two types of alums (aluminium sulfate) by dividing the alumina leaching process into two steps. In the first step, leaching was carried out with dilute H_2SO_4 to remove impurities, and in the second step, alumina was extracted from the purified dross tailings using concentrated H_2SO_4 [14]. El-Katatny et al. [26] described a process where aluminium can be recovered from dross by precipitating aluminium hydroxide using a NaOH solution. The aluminium hydroxide powder is then activated at 600°C to obtain γ-Al_2O_3.

Radioactive wastewater is documented as a very risk hazardous material and the main sources of this waste are the radioactive isotopes. Radioactive isotopes are continuous sources for radiations like beta and gamma [27]. In addition to the previous, ^{60}Co radioactive isotopes are known as hazardous radioactive isotopes which produce gamma rays with the high possibility of penetration into the human body to cause internal irradiation in the human cells and may lead to the death [28].

The main aims of the present study is (i) to prepare purified alumina from AD by different dissolution methods, (ii) to optimize the condition required for the effective removal of radioactive cobalt from waste solution by means of batch adsorption experiments and (iii) to convert AD waste to high value materials and minimize its environmental impact.

2. Materials and methods

2.1. Materials and reagents

AD is a waste material and was obtained from the Egyptalum Company, Nag Hammady, Egypt. The H_2SO_4, HCl and NaOH used in the AD leaching experiments were analytical grade reagents (Merck Company, Germany).

2.2. Acidic leaching of AD

First, 313.7 g of AD was added to 400 ml concentrated sulfuric acid at 90°C, and 100 ml of 1 N sulfuric acid was added to complete digestion. As the dissolution reaction is exothermic, the temperature of the leaching medium spontaneously increased up to 80°C–85°C. A hot plate was utilized to maintain the temperature at 90°C ± 2°C. A paste was formed and then dissolved in 7 L of hot distilled water at 70°C. The pH of the solution was 1.5. The leach solution obtained (soluble aluminium sulfate), after filtration, was subjected to

direct precipitation using 50% aqueous ammonia that was added dropwise. The resulting pH was 7. The produced gel was left to stand for 2 h (aging time) in the mother liquor at 80°C. Following the ageing step, the gel was washed until no additional sulfate ions were detected in the washings. Finally, the gel was dried at 60°C for 24 h, ground and calcined for 3 h in a muffle furnace in air at 500°C, 700°C and 900°C.

During the sulfuric acid leaching of the dross, all the aluminium present in the dross was converted to water-soluble aluminium sulfate, as shown in the following reaction.

2.3. Leaching of AD by NaOH

20 g of aluminium slag was dissolved in 50 ml 2 N NaOH (exothermic reaction accompanied by effervescence). The solution sat overnight under vigorous stirring at 80°C. The pH of the solution was 10.8. The resulting solution (soluble sodium aluminate, $Na[Al(OH)_4]_{(aq)}$) was divided into two aliquots. The first one was neutralized by dropwise addition of 2 N H_2SO_4 until a white precipitate formed at pH 8. The precipitate was washed by distilled water. The second part of the solution was neutralized by dropwise addition of 2 N HCl until a white precipitate formed at pH 7. The precipitate was washed by distilled water. The two precipitates were dried at 85°C and calcined in air at 700°C.

2.4. Characterization

Chemical analyses of the AD and prepared materials were performed using a Philips sequential X-ray fluorescence (XRF) spectrometer (2400). X-ray diffraction (XRD) patterns were recorded at room temperature using a powder diffractometer (Bruker Axis D8 Advance, Germany) with a Cu-Kα radiation source, λ = 1.5406 Å and 2θ in the range of 10°–80°. The average crystallite size of the nanoparticles was determined according to the Scherrer equation [29].

$$D = \frac{0.9\lambda}{\left(\beta \cos \theta\right)} \tag{1}$$

where λ is the X-ray wavelength, θ is the Bragg angle of the peak of interest and β is the line broadening measured from the peak width at half height. The porous structure of alumina was characterized by adsorption–desorption of N_2 Brunauer–Emmett–Teller (BET method) at the temperature of liquid nitrogen (77 K) (JEOL-JSM 6510 LA, Japan). Scanning electron microscopy (SEM) was used to examine the pore structure of the prepared aluminium samples.

2.5. Adsorption study

The radioisotope (^{60}Co) used in this study was supplied by Hot Laboratories and Waste Management Centre (HLWMC)-Egyptian Atomic Energy Authority (EAEA). A ^{60}Co solution with high specific activity was used as a tracer. The radioactive ^{60}Co tracer was measured by a NaI scintillation detector connected to a multi-channel analyser (Genne 2000, USA). Stock solutions of 1,000 mg L^{-1} Co(II) in distilled water were prepared from the salt precursor $CoCl_2{\cdot}(H_2O)_6$. The ^{60}Co tracer was mixed with known amounts of inactive cobalt chloride to obtain cobalt concentrations in the range of 100–500 ppm. Batch experiments were conducted with different shaking times of 15, 30, 60, 120, 180 and 1440 min at 25°C. The adsorption isotherms were obtained under the optimum conditions for the adsorption of Co. The effect of the initial pH of the Co solution on the sorption process was investigated at pH values of 2, 4, 6 and 8.

After reaching equilibrium, the solid/liquid phases were separated by centrifugation (4,000 rpm). For the adsorption of contaminants, the adsorption capacity q_e (mg of adsorbate/g of adsorbent) of the adsorbent was calculated as follows:

$$q_e = \frac{V \times \left(C_i - C_e\right)}{m} \tag{2}$$

where C_i is the initial concentration of the metal in solution (in mg L^{-1}), C_e is the metal concentration at equilibrium, V is the volume of solution in litres, and m is the weight of the adsorbent in grams.

The uptake percent (U %) of Co^{2+} was calculated by the following equation:

$$U\% = \frac{\left(A_0 - A\right)}{A_0} \times 100 \tag{3}$$

where A_0 and A are the activities expressed in counts per minute of the radioisotope in a 2 mL solution before and after contact with the prepared aluminium samples.

3. Results and discussion

The synthesis processes of Al_2O_3 from AD through acid and base leaching are summarized in Fig. 1. During sulphuric acid leaching of the dross, all the aluminium presented in dross converted to water-soluble aluminium sulphate (AS) as shown in the following equations:

$$Al_2O_3 + 3H_2SO_4 = Al_2\left(SO_4\right)_3 + 3H_2O \tag{4}$$

$$2Al + 3H_2SO_4 = Al_2\left(SO_4\right)_3 + 3H_2 \tag{5}$$

$$2Al + 6H_2SO_4 = Al_2\left(SO_4\right)_3 + 3SO_2 + 6H_2O \tag{6}$$

On the other hand, the alkali leaching process is based on dissolution of Al and Al_2O_3 in strong sodium hydroxide solution at atmospheric condition. Aluminium can be recovered as aluminium hydroxide by precipitation. Alumina can be then produced by calcination at high temperature as shown in the following equations [30,31].

$$Al_2O_3 + 2NaOH \rightarrow 2NaAlO_2 + H_2O \tag{7}$$

$$2Al + 2NaOH + 2H_2O \rightarrow 2NaAlO_2 + 3H_2 \uparrow \tag{8}$$

$$NaAlO_2 + HCl + H_2O = Al\left(OH\right)_3 \downarrow + NaCl \tag{9}$$

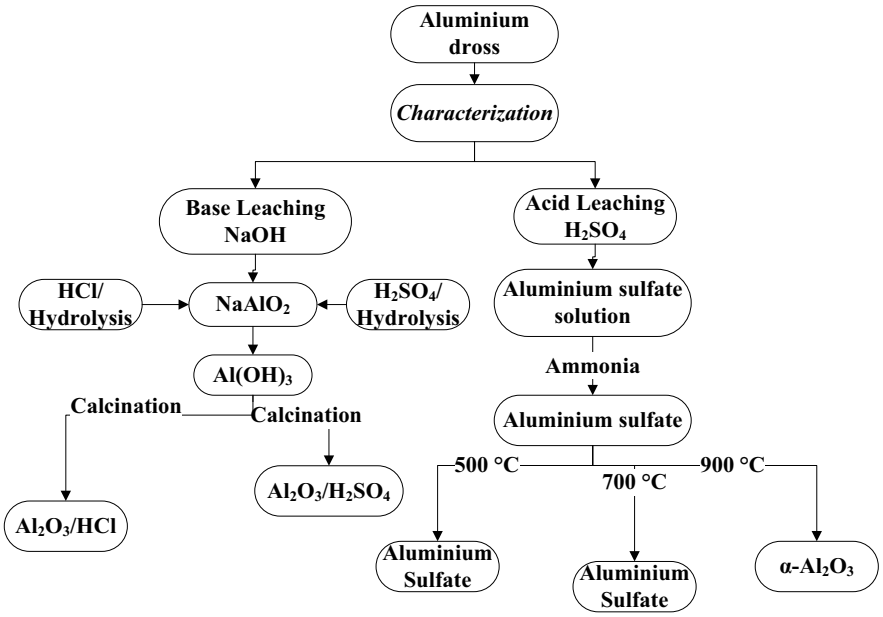

Fig. 1. Flow chart for the synthesis of Al_2O_3 from aluminium dross through acid and base leaching.

$$NaAlO_2 + H_2SO_4 + H_2O = Al(OH)_3 \downarrow + Na_2SO_4 \quad (10)$$

$$2Al(OH_3) + \text{heat} \rightarrow Al_2O_3 + 3H_2O \quad (11)$$

3.1. Characterization

The chemical composition of the AD is given in Table 1. The XRF analysis of the AD, AS, α-alumina, alumina/HCl and alumina/H_2SO_4 (expressed in concentration percentages). The results indicated that highly pure alumiuim oxide samples can be obtained. The concentrations of Al analyet increased from 92.355% in AD to 98.794, 97.599 and 96.394 for α-AO, AO/HCl and AO/H_2SO_4. Some trace elemental oxides of Ca, Ti and Zr were detected in AD and disappeared in aluminum oxides samples.

The XRD pattern of the AD is shown in Fig. 2. The AD contained corundum or α-alumina (Al_2O_3, 49.2%), calcium AO (38.1%) and AO (12.7%).

Solubility of the black dross in sulfuric acid can be determined from the initial weight of dross and dry residue. During sulfuric acid digestion, 70% of Al dross was dissolved at 80°. Fig. 3 shows the XRD pattern of the as-prepared Al sample after acid digestion and precipitation at pH 7 by 30% ammonium hydroxide at room temperature. The sample contains three compounds, Tohdite ($5Al_2O_3 \cdot H_2O$, 48.3%), aluminium chloride hydrate ($AlCl_3$ $(H_2O)_6$, 13.1%), and aluminium hydrogen sulphate hydrate ($Al(HSO_4)_3 \cdot 6H_2O$, 38.6%). Calcium AO was not detected in the prepared aluminium sample. The detected chloride is mainly attributed to the high chloride concentration in the original dross (NaCl). In this respect, the prepared sample was not washed enough.

XRD analysis (Fig. 4) confirms the transformation of Tohdite, aluminium hydrogen sulphate hydrate and aluminium chloride hydrate into alumina (α-Al_2O_3 or corundum) by calcination of the resulted sample from acid leaching at 900°C.

Table 1
XRF analyses of aluminium slag and the treated AO samples

Analyte	Concentration				
	Dross	Aluminium sulfate	α-AO	AO/HCl	AO/H_2SO_4
Al	92.355	47.729	98.794	97.599	96.394
Si	1.301	0.714	0.473	2.011	2.097
S	1.069	50.136	0.411	0.39	1.509
Cl	0.212	0.24	0.123		
Ca	0.578	0.177			
Ti	0.13	0.108			
Zr	0.018	0.894			

3.2. Effect of the calcination temperature on aluminium sample morphology

To study the effect of the calcination temperature on the aluminium sulfate morphology, the prepared sample from H_2SO_4 digestion was calcined at 500°C, 700°C and 900°C. Fig. 5 shows the effect of calcination temperature on the as prepared aluminium hydrogen sulphate. The XRD results indicated that aluminium hydrogen sulfate was stable up to 700°C. At 900°C, the as-prepared aluminium hydrogen sulfate was converted to α-Al_2O_3. Alumina powders were produced from the conversion of the $Al_2(SO_4)_3$ at high temperatures. $Al_2(SO_4)_3 \cdot 18H_2O$ is a complex molecule. Calcinations on the $Al_2(SO_4)_3 \cdot 18H_2O$ break down the bond in the complex molecule and provide sufficient interaction for the elements to form a new compound that is simpler and more stable. At sufficiently high calcination temperatures, $Al_2(SO_4)_3 \cdot 18H_2O$

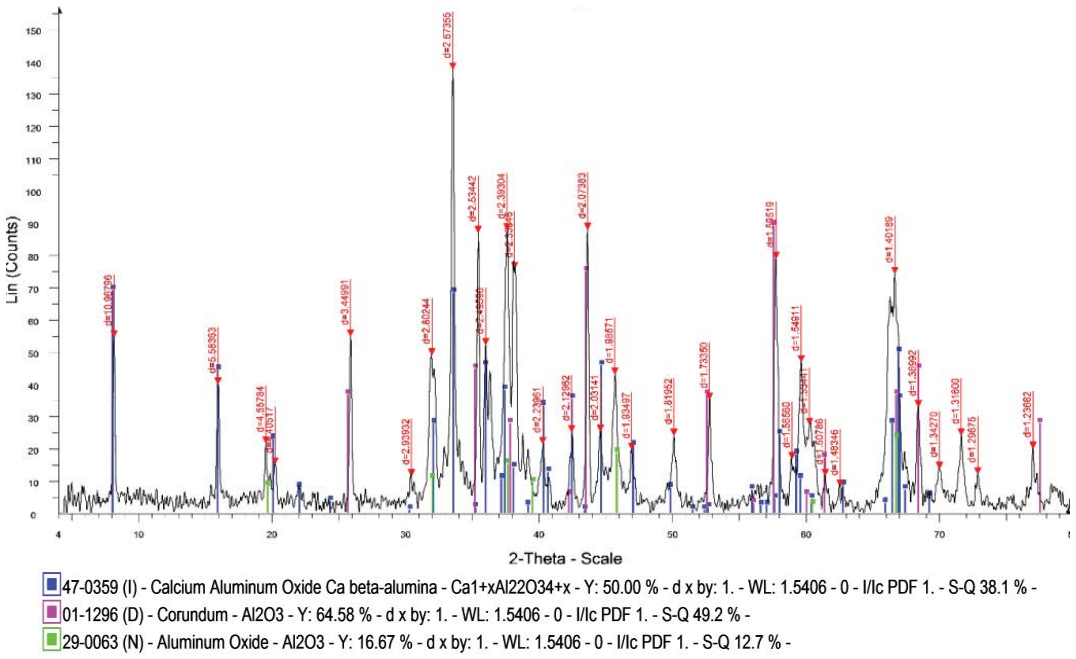

Fig. 2. XRD patterns of the original dross

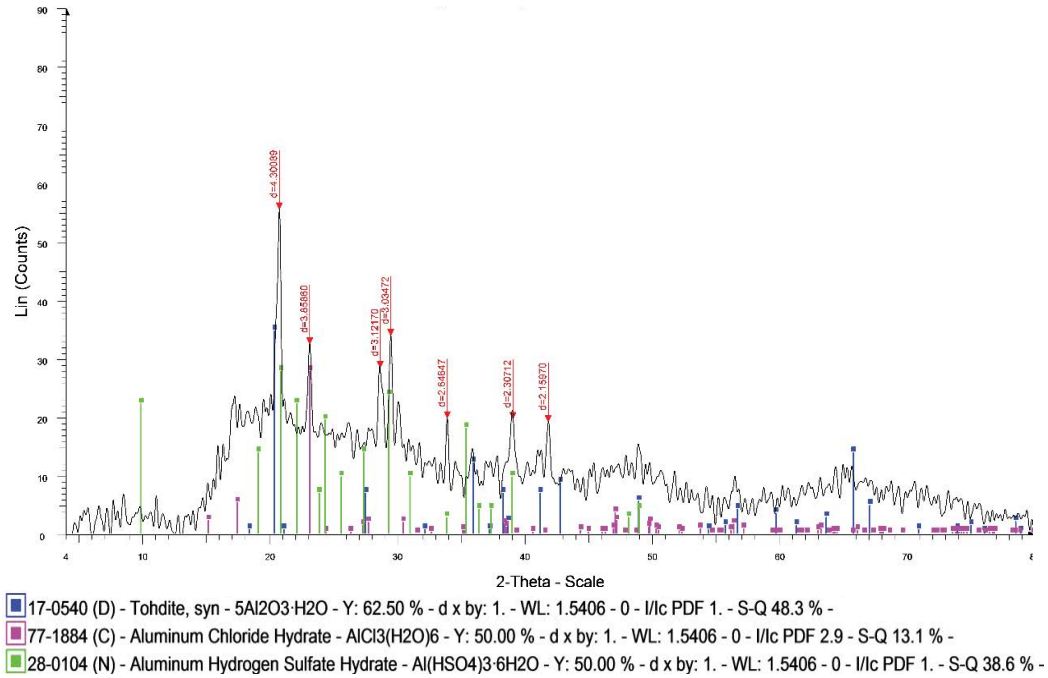

Fig. 3. XRD pattern of the as-prepared Al sample after acid digestion.

is fully converted into alumina by eliminating water vapor, followed by the elimination of sulfur trioxide gas; these reactions are shown in Eqs. (12) and (13) [32–34]. Some volatile impurities in the gaseous state are also driven off. The calcinations provide heat energy to the alumina, which is needed for it to undergo further phase transformations to form α-alumina, the most stable crystalline structure of alumina.

$$Al_2(SO_4)_3 \times 18H_2O(s) \rightarrow Al_2(SO_4)_3(s) + 18H_2O(g) \quad (12)$$

$$Al_2(SO_4)_3(s) \rightarrow Al_2O_3(s) + 3SO_3(g) \quad (13)$$

These results indicate that 900°C is sufficient to form AO crystals and activate AO by eliminating most of the water. Also,these results confirm the presence of impurities alters the barrier of phase transformations. In the previous studies, calcinations of γ-Al_2O_3 with 3% platinum impurity can cause the α-Al_2O_3 to form below 1,100°C [23–25]. The XRD

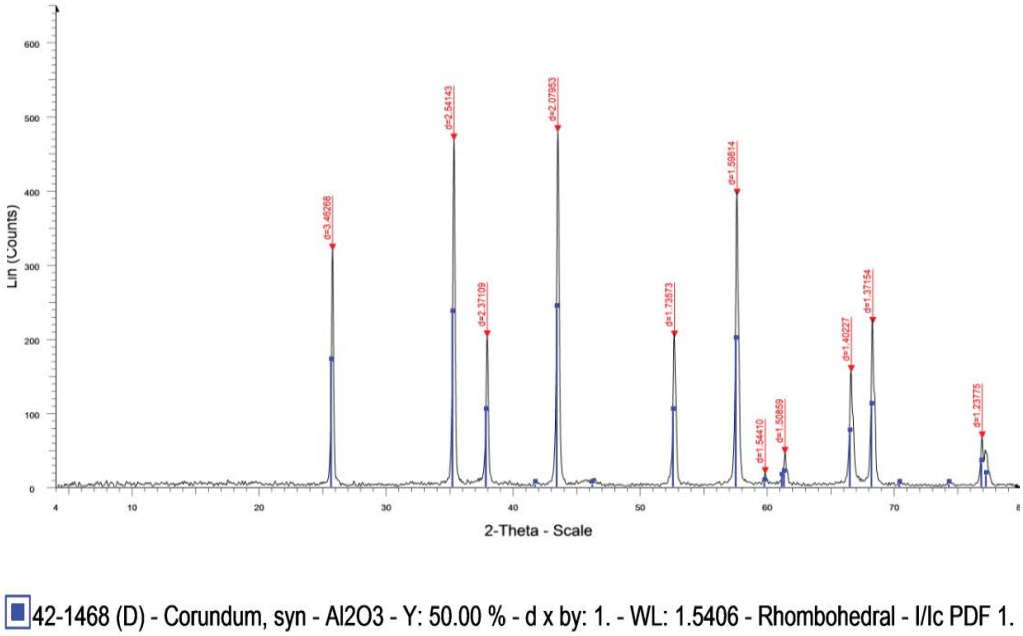

Fig. 4. XRD pattern of alumina synthesized from AD leachate of H_2SO_4 calcined at 900°C.

results from Table 2, related to Fig. 5, confirm the presence of α-Al_2O_3

3.3. AD leaching using NaOH

Fig. 6 illustrates the XRD patterns of alumina (Al_2O_3/H_2SO_4, Al_2O_3/HCl) from the NaOH leachate and neutralized by acid (2 N H_2SO_4 and 2 N HCl). The as-prepared aluminium hydroxide (boehmite) was heat treated at 700°C to obtain γ-Al_2O_3, which is a high-value activated alumina form that can be used as an adsorbent. Table 1 shows the XRF analysis for the alumina samples after base leaching and neutralized by H_2SO_4 and HCl. The result confirm the increasing the concentration of alumina and decreasing the content of impurities and salts.

3.4. Surface area results

The BET specific surface area, pore diameter and pore volume of the different aluminium samples were obtained. The BET analysis results for the synthesized aluminium samples are summarized in Table 4. A comparison of the surface areas of the samples as a function of the calcination temperature showed that the surface area of AD was 1.274 m^2 g^{-1} and increased to 9.341 m^2 g^{-1} after acid digestion. The α-Al_2O_3 calcined at 900°C had a surface area of 36.466 m^2 g^{-1}. Based on these results, H_2SO_4 leaching of AD increases the surface area, pore volume and pore diameter of the resulting material, as shown in Table 4. These improvements in the surface area and pore volume reflect the efficient expected uses of alumina (α-Al_2O_3) as sorbent for hazardous metals removal.

3.5. SEM results

Fig. 7 shows the images of the as-synthesized aluminium sulfate, alumina calcined at 900°C, alumina/HCl and alumina/H_2SO_4. The morphologies of the samples appear to be lumpy, consisting of dense aggregates of lumpy amorphous macro-crystallites. The micro-crystallites appeared to be very small, that is, in the nano-size range; the actual crystal size could not be determined from the SEM images. Additionally, all samples show significant differences in terms of shape and size uniformity.

Table 2
XRD diffraction data of resulted α-Al_2O_3 calcined at 900°C

Position	Area	Cry size L(nm)	Peak identity
25.68311	74.53126	91.8	α-Al_2O_3
35.2535	121.2017	90.1	α-Al_2O_3
37.87103	57.45199	73.2	α-Al_2O_3
43.45542	132.9412	94.3	α-Al_2O_3
52.63905	64.02469	88.3	α-Al_2O_3
57.58051	130.3576	83.6	α-Al_2O_3
59.81626	5.739617	53.4	α-Al_2O_3
61.34287	17.59781	45.9	α-Al_2O_3
66.59101	62.9386	63.3	α-Al_2O_3
68.27992	78.41881	87	α-Al_2O_3
76.99669	32.73482	52.3	α-Al_2O_3

4. Sorption study

4.1. Effect of shaking time

The effect of shaking time on radioactive Co^{2+} distribution is tested to clarify its insights into reaction kinetics. The sorption kinetics of radioactive Co^{2+} was studied at different time intervals ranging from 10 min to 24 h at constant V/M (0.1 L g^{-1}) ratio. As shown in Figs. 8 and 9, the equilibrium

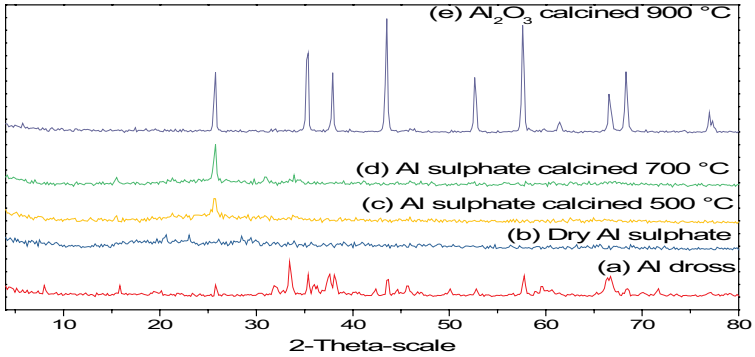

Fig. 5. XRD patterns of (a) AD, (b) prepared aluminium sulphate, (c) aluminium sulfate calcined at 500°C, (d) aluminium sulfate calcined at 700°C and (e) aluminium oxide calcined at 900°C.

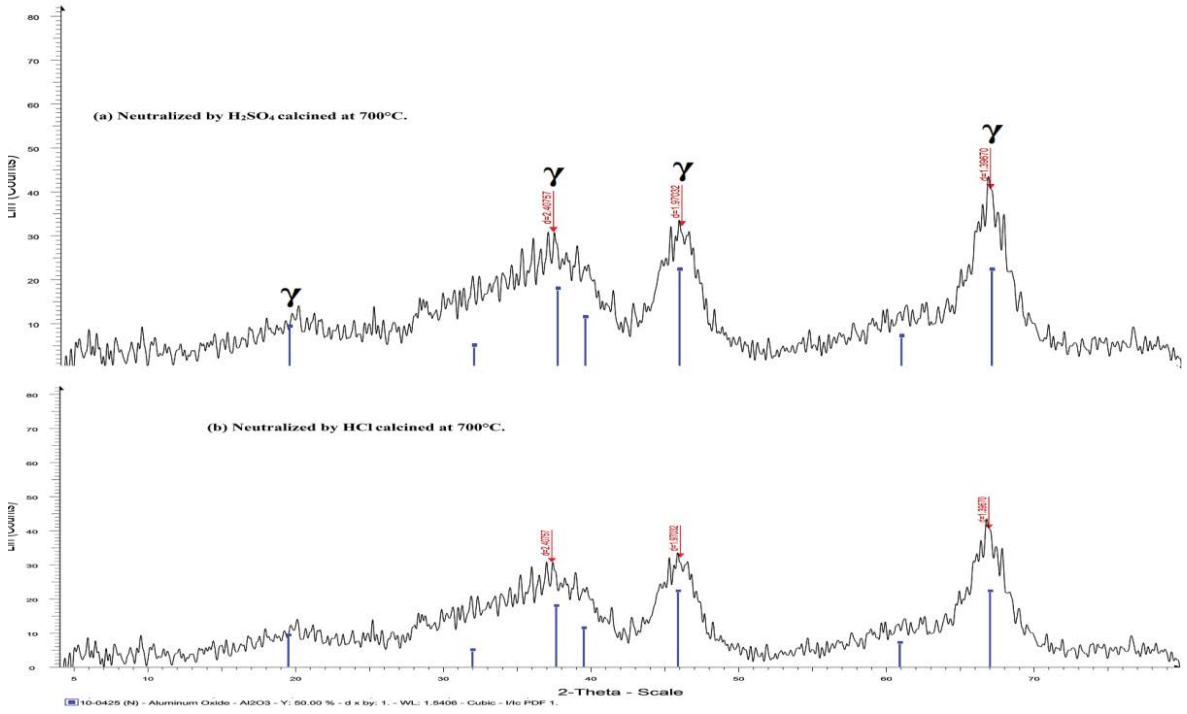

Fig. 6. XRD patterns of alumina synthesized from Al dross leached by NaOH (a) neutralized by H_2SO_4 calcined at 700°C and (b) neutralized by HCl calcined at 700°C.

Table 3
Summary of the results for the aluminium samples at different stages (acid leaching) based on the XRD results

Sample name	Compound name
Aluminium dross	Calcium aluminium oxide
	Corundum or α-alumina, Al_2O_3
	Aluminium oxide
Dried Al sample after acid digestion and sulfate hydrolysis	Tohdite, aluminium oxide hydroxides, $5Al_2O_3{\cdot}H_2O$
	Aluminium chloride hydrate, $AlCl_3(H_2O)_6$
	Aluminium hydrogen sulfate hydrate- $Al(HSO_4)_3{\cdot}6H_2O$
Al sample after acid digestion calcined at 500°C	$Al_2(SO_4)_3$
Al sample after acid digestion calcined at 700°C	$Al_2(SO_4)_3$
Al sample after acid digestion calcined at 900°C	Alumina, α-Al_2O_3

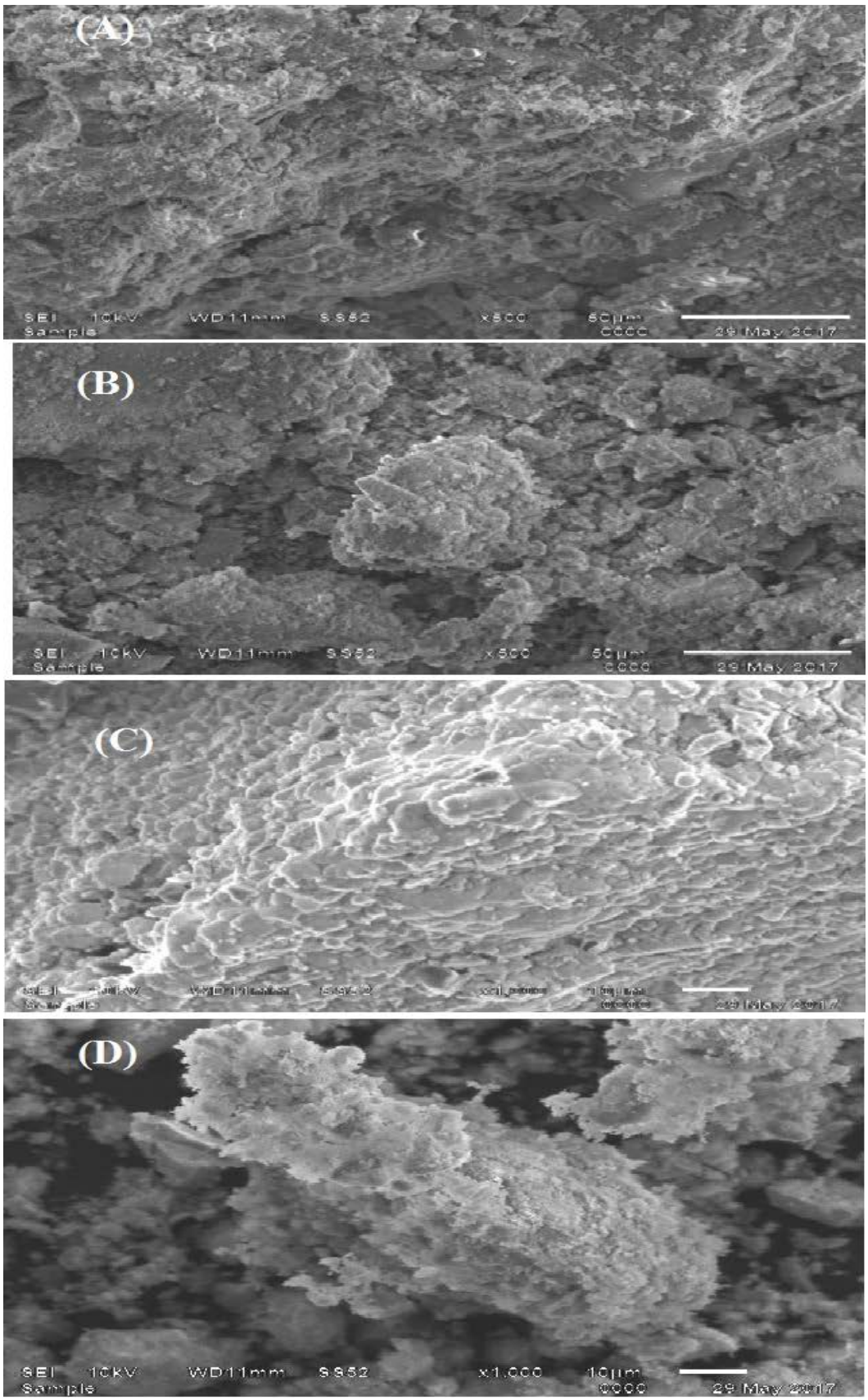

Fig. 7. SEM images of (a) synthesized aluminium sulphate, (b) alumina calcined at 900°C, (c) alumina/HCl and (d) alumina/H_2SO_4.

Table 4
Results of the BET analyses of aluminium samples for nitrogen adsorption–desorption (S_{BET}) and crystallite size (XRD)

Sample	Specific surface area ($m^2 g^{-1}$)	Average pore radius	Total pore volume (cc/g)	Mean crystallite size (nm)
Aluminium dross	1.274	192.162	0.01224	54
Al originally prepared	9.341	100.00512	0.04695	22
α-Al_2O_3 calcined at 900°C	36.466	60.31627	0.1152	75

time for radioactive Co^{2+} on the originally prepared AS, alumina calcined at 700°C, alumina calcined at 900°C, alumina/HCl and alumina/H_2SO_4 is reached at 2 h. As shown in Fig. 8, it could be observed that, at pH 4, the sorption uptake of Co(II) increases from ~17% to ~51%, ~7% to ~33% and ~92% to ~98% for Al-sulphate, Al-sulphate calcined at 700°C and alumina calcined at 900°C, respectively.

For the alumina resulted from base leaching the sorption of Co(II) on alumina/HCl and alumina/H_2SO_4 increases from ~93% to ~98% and ~92% to ~97% respectively, of the initial concentration respectively of Co(II) at pH 4, (Fig. 9). The fast sorption process at initial stage could be attributed to fact that large number active sites are available for sorption on to aluminium sample.

4.2. Effect of pH on the sorption process

To assess the effect of pH on adsorption, experiments were performed at different pH values ranging from 2 to 8 with active Co^{2+} ions and a contact time of 120 min. This pH

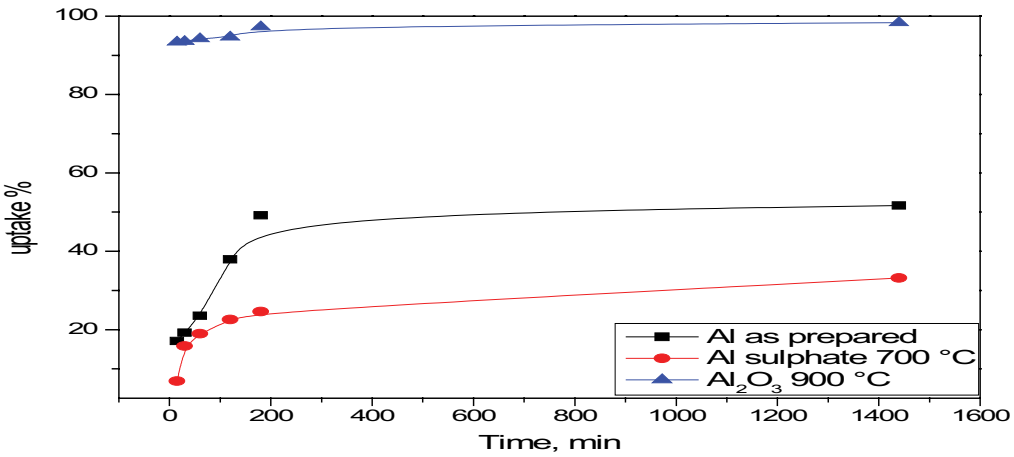

Fig. 8. Effect of contact time on the adsorption of radioactive Co^{2+} on the as-synthesized alumina, alumina calcined at 700°C and alumina calcined at 900°C; adsorbent dosage: 10 g L^{-1}.

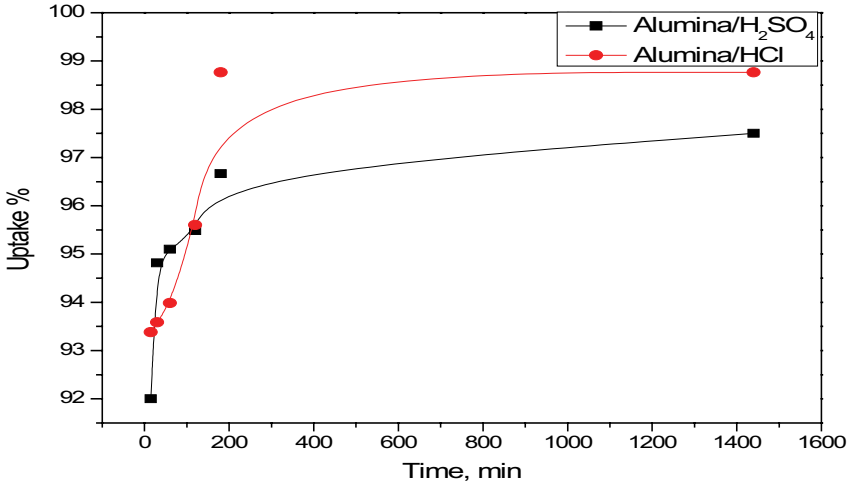

Fig. 9. Effect of contact time on the adsorption of radioactive Co^{2+} on alumina/HCl and alumina/H_2SO_4 from base digestion; adsorbent dosage: 10 g L^{-1}.

range was selected to avoid metal hydrolysis. Figs. 10 and 11 showed the effect of pH on the adsorption of radioactive Co^{2+} on the as-synthesized aluminium sulfate, aluminium sulfate calcined at 700°C and alumina calcined at 900°C, alumina/HCl and alumina/H_2SO_4 (from base leaching). As expected, higher acidity conditions led to lower adsorption of metal ions, which may be due to protonation of functional groups. As the pH of the solution increased, adsorption increased due to deprotonation of functional groups on all alumina samples. When the pH decreased, competitive adsorption occurred between H^+ ions and the radioactive Co^{2+} ions in solution. Therefore, the uptake increased as the pH increased, and the maximum uptake was observed at pH 4 for radioactive Co^{2+}.

4.3. Maximum retention capacity of Co^{2+}

As shown in Fig. 12, the retention capacity of Co^{2+} ions by the as-synthesized aluminium sulfate, AS calcined at 700°C, alumina calcined at 900°C, alumina/HCl and alumina/H_2SO_4 as a function of their concentration ranged from 100 to 500 mg L^{-1} at the corresponding optimum pH (pH 4). The equilibrium capacity of Co^{2+} ions increased as increasing amounts of metal ions were added. The maximum Co^{2+} adsorption capacity was 193, 180, 197, 296 and 235 mg g^{-1} for the as-synthesized alumina, alumina calcined at 700°C, alumina calcined at 900°C, alumina/HCl and alumina/H_2SO_4, respectively. This means that the alkaline digestion of AD followed by acidic neutralization (HCl or H_2SO_4) provided efficient adsorbents with higher retention capacities than that of acidic digestion. Therefore, both alumina/HCl and alumina/H_2SO_4 could be applied for efficient removal of radio-cobalt ions from radioactive liquid waste.

5. Conclusion

Alumina as useful sorbent material can be recovered from environmental hazard AD by acidic or alkaline digestion process. The process developed for the treatment of AD. The treatment dissolution processes by H_2SO_4 or NaOH

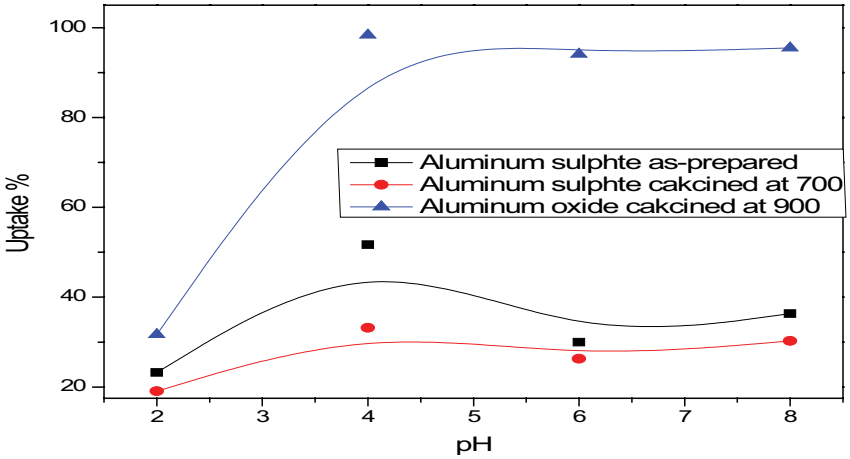

Fig. 10. Effect of pH on the adsorption of radioactive Co^{2+} on the as-synthesized aluminium sulfate, aluminium sulphate calcined at 700°C and alumina calcined at 900°C; adsorbent dosage: 10 g L^{-1}.

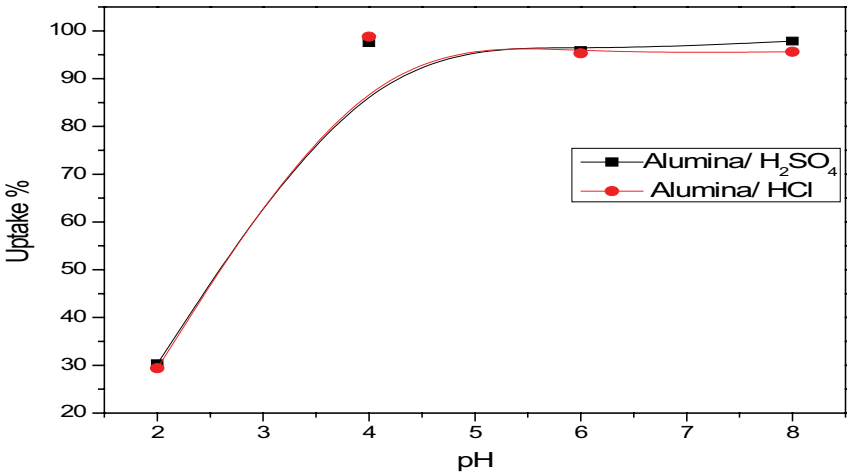

Fig. 11. Effect of pH on the adsorption of radioactive Co^{2+} on alumina/HCl and alumina/H_2SO_4 from base digestion; adsorbent dosage: 10 g L^{-1}.

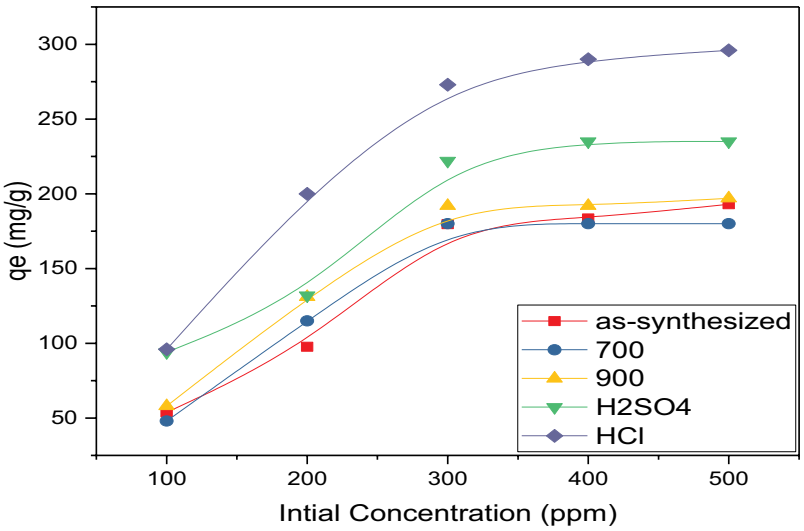

Fig. 12. Sorption isotherm of Co^{2+} ions on different aluminium samples at pH 4, V/M = 0.1 L g^{-1}.

have been optimized to remove radioactive cobalt from aqueous waste. The maximum Co^{2+} adsorption capacities were found to be 193, 180, 197, 296 and 235 mg g^{-1} for the synthesized Al-sulphate, alumina calcined at 700°C, alumina calcined at 900°C, alumina/HCl and alumina/H_2SO_4, respectively. Finally, the results showed that both alumina/HCl and alumina/H_2SO_4 are efficient and promising adsorbents for removal of radio-cobalt ions from radioactive liquid waste.

References

[1] T.W. Unger, M. Beckmann, Salt Slag Processing for Recycling, The 121st TMS Annual Meeting, San Diego, CA, USA, 03/01-05/92, 1991, pp. 1159–1162.

[2] J.A.S. Tenorio, D.C.R. Espinosa, Effect of salt/oxide interaction on the process of aluminum recycling, J. Light Met., 2 (2002) 89–93.

[3] B. Dash, B. Tripathy, I. Bhattacharya, S. Das, C. Mishra, B. Pani, Effect of temperature and alumina/caustic ratio on precipitation of boehmite in synthetic sodium aluminate liquor, Hydrometallurgy, 88 (2007) 121–126.

[4] N. Murayama, J. Shibata, K. Sakai, S. Nakajima, H. Yamamoto, Synthesis of hydrotalcite-like materials from various wastes in aluminum regeneration process, Resour. Process., 53 (2006) 6–11.

[5] J. Shibata, N. Murayama, M. Tanabe, H. Yamamoto, Synthesis of hydrotalcite from wastes discharged in aluminum regeneration process and its physical properties, Kagaku Kogaku Ronbunshu, 31 (2005) 74–79.

[6] J. Shibata, Method to produce layered double hydroxide, Japanese Patent Disclosure, H06-151744, (2006).

[7] N. Murayama, N. Okajima, S. Yamaoka, H. Yamamoto, J. Shibata, Hydrothermal synthesis of AlPO 4-5 type zeolitic materials by using aluminum dross as a raw material, J. Eur. Ceram. Soc., 26 (2006) 459–462.

[8] N. Murayama, K. Arimura, N. Okajima, J. Shibata, Effect of structure-directing agent on AlPO 4-n synthesis from aluminum dross, Int. J. Miner. Process., 93 (2009) 110–114.

[9] N. Murayama, H. Yamamoto, J. Shibata, Synthesis of hydrotalcite and its anion exchange properties, Resour. Process., 51 (2004) 92–98.

[10] N. Murayama, M. Tanabe, R. Shibata, H. Yamamoto, J. Shibata, Removal of toxic heavy metal ions in aqueous solution with Mg/Al type hydrotalcite derived from wastes, Kagaku Kogaku Ronbunshu, 31 (2005) 285–290.

[11] E.A. EI-Katatny, S.A. Halawy, M.A. Mohamed, M.I. Zaki, Recovery of high surface area alumina from aluminium dross tailings, J. Chem. Technol. Biotechnol., 75 (2000) 394–402.

[12] M. Barakat, S. El-Sheikh, F. Farghly, Regeneration of spent alkali from aluminum washing, Sep. Purif. Technol., 46 (2005) 214–218.

[13] B. Dash, B. Das, B. Tripathy, I. Bhattacharya, S. Das, Acid dissolution of alumina from waste aluminium dross, Hydrometallurgy, 92 (2008) 48–53.

[14] A. Amer, Extracting aluminum from dross tailings, J. Miner. Metals Mater. Soc., 54 (2002) 72–75.

[15] G.-F. Fu, W. Jing, K. Jian, Influence of AlF_3 and hydrothermal conditions on morphologies of α-Al_2O_3, Trans. Nonferrous Met. Soc. China, 18 (2008) 743–748.

[16] F. Habashi, Principles of Extractive Metallurgy, Volume 2, Hydrometallurgy, Gordon & Breach, New York, 1970.

[17] E. Borai, M. Eid, H. Aly, Determination of REEs distribution in monazite and xenotime minerals by ion chromatography and ICP-AES, Anal. Bioanal. Chem., 372 (2002) 537–541.

[18] Y. Wang, C. Suryanarayana, L. An, Phase transformation in nanometer-sized γ-alumina by mechanical milling, J. Am. Ceram. Soc., 88 (2005) 780–783.

[19] J.F. Shackelford, R.H. Doremus, Ceramic and Glass Materials, JF Shackelford, RH Doremus, 2008.

[20] C.-K. Loong, J. Richardson Jr., M. Ozawa, Structural phase transformations of rare-earth modified transition alumina to corundum, J. Alloys Compd., 250 (1997) 356–359.

[21] O. Mekasuwandumrong, P. Tantichuwet, C. Chaisuk, P. Praserthdam, Impact of concentration and Si doping on the properties and phase transformation behavior of nanocrystalline alumina prepared via solvothermal synthesis, Mater. Chem. Phys., 107 (2008) 208–214.

[22] P. Bowen, C. Carry, From powders to sintered pieces: forming, transformations and sintering of nanostructured ceramic oxides, Powder Technol., 128 (2002) 248–255.

[23] W. Gitzen, Alumina as a Ceramic Material, American Ceramic Society, Inc., Columbus, OH, 17, 1970.

[24] P. Mishra, Low-temperature synthesis of α-alumina from aluminum salt and urea, Mater. Lett., 55 (2002) 425–429.

[25] D.J. Young, High Temperature Oxidation and Corrosion of Metals, Elsevier, 2008.

[26] E.A. El-Katatny, S.A. Halawy, M.A. Mohamed, M.I. Zaki, Surface composition, charge and texture of active alumina powders recovered from aluminum dross tailings chemical waste, Powder Technol., 132 (2003) 137–144.

[27] M.E. Mahmoud, M.A. Khalifa, Y.M. El Wakeel, M.S. Header, T.M. Abdel-Fattah, Engineered nano-magnetic iron oxide-

urea-activated carbon nanolayer sorbent for potential removal of uranium (VI) from aqueous solution, J. Nucl. Mater., 487 (2017) 13–22.
[28] E. Borai, M. Breky, M. Sayed, M. Abo-Aly, Synthesis, characterization and application of titanium oxide nanocomposites for removal of radioactive cesium, cobalt and europium ions, J. Colloid Interface Sci., 450 (2015) 17–25.
[29] P. Scherrer, Estimation of the size and internal structure of colloidal particles by means of röntgen, Nachr. Ges. Wiss. Göttingen, 2 (1918) 96–100.
[30] H.-K. Park, H.-I. Lee, E.-P. Yoon, Process for Recycling Waste Aluminum Dross, Google Patents, 2001.
[31] J.W. Pickens, M.D. Waite, Recovery of Products from Non-metallic Products Derived from Aluminum Dross, Google Patents, 2000.
[32] J. Kloprogge, J. Geus, J. Jansen, D. Seykens, Thermal stability of basic aluminum sulfate, Thermochim. Acta, 209 (1992) 265–276.
[33] I. Bhattacharya, P. Gochhayat, P. Mukherjee, S. Paul, P. Mitra, Thermal decomposition of precipitated low bulk density basic aluminium sulfate, Mater. Chem. Phys., 88 (2004) 32–40.
[34] N. Apte, E. Kiran, J. Chernosky, Thermal decomposition of aluminium-bearing compounds, J. Therm. Anal., 34 (1988) 975–981.